Journal of Applied Polymer Science

Effects of silanization temperature and silica type on properties of silica-filled solution styrene butadiene rubber (SSBR) for passenger car tire tread compounds

Puchong Thaptong,[1,2] Pongdhorn Sae-Oui,[2,3] Chakrit Sirisinha[1,3]

[1]Department of Chemistry, Faculty of Science, Mahidol University, Rama VI Rd, Rajdhevee, Bangkok 10400, Thailand

[2]MTEC, National Science and Technology Development Agency, 114 Thailand Science Park, Paholyothin Rd, Klong 1, Klong-Luang, Pathumthani 12120, Thailand

[3]Rubber Technology Research Centre (RTEC), Faculty of Science, Mahidol University, Phutthamonthon 4 Rd, Salaya, Nakornprathom 73170, Thailand

Correspondence to: C. Sirisinha (E-mail: chakrit.sir@mahidol.ac.th)

ABSTRACT: Influence of silanization temperature on properties of silica-filled solution polymerized styrene butadiene rubber was investigated. Two types of silica, i.e., highly dispersible silica (HDSi) and conventional silica (CSi), were compared. Results show that the increased silanization temperature leads to the enhanced rubber–filler interaction, filler dispersion, and cross-link density giving rise to the improvement in vulcanizate properties such as modulus, heat build-up (HBU), and dynamic set, as well as tire performance, e.g., wet grip (WG), rolling resistance (RR), and abrasion resistance. Great care, however, must be taken to avoid the scorching phenomenon during the mixing process at too high temperature. Taken as a whole, the balanced properties are found at the silanization temperature of 140°C. Surprisingly, HDSi provides insignificant differences in degree of filler dispersion, WG, and RR, compared to CSi, despite its claimed greater dispersability. Probably, the relatively long mixing time used in this experiment may override the influence of silica type. © 2016 Wiley Periodicals, Inc. J. Appl. Polym. Sci. **2016**, *133*, 43342.

KEYWORDS: elastomers; mechanical properties; rubber; synthesis and processing; viscosity and viscoelasticity

Received 17 September 2015; accepted 11 December 2015

DOI: 10.1002/app.43342

INTRODUCTION

Tread is one of the most important parts of tire because it is the outer part of tire that contacts the road surface, and protects the inner casing from road hazards. Apart from tread pattern, tire performance depends strongly on tire tread properties.[1] Generally, tire performance is evaluated based on three main properties namely "the magic triangle", i.e., fuel efficiency related to the rolling resistance (RR),[2] wet grip (WG) corresponding to an efficiency of car control and breaking performance on a wet road,[3] and wear resistance.

Many attempts have been made to investigate the properties of tire tread compounds based on carbon black (CB),[4,5] silica,[4,6–8] CB/silica hybrid filler,[4,9–11] and CB/clay hybrid filler.[12,13] It has been reported that the replacement of CB by silica in passenger car tire tread leads to a significantly reduced RR without sacrificing WG and wear resistance.[14] Unlike CB, silica surfaces are densely covered by silanol groups (-Si-O-H) which can facilitate strong transient filler network formation through intermolecular hydrogen bonding,[15] leading to the difficulty to achieve good filler dispersion. Moreover, because of its hydrophilic nature, silica is less compatible with most rubbers used in the production of tire tread such as natural rubber (NR), styrene butadiene rubber (SBR), and butadiene rubber (BR), leading to negative effect on tire performance. However, after the advent of silane coupling agents (SCAs), silica has become more popular in tire industry. It has been reported that the addition of organosilane, e.g., bis-(3-(triethoxysilyl)-propyl)-tetrasulfide (TESPT), into silica-filled rubber, not only improves silica dispersion but also enhances rubber–silica interaction leading to the improvement in RR and WG.[16] To gain maximum benefit from SCAs, the reaction between silanol groups on silica surfaces and alkoxy groups of SCAs, so-called silanization, must take place sufficiently during the mixing process. Several attempts have been made to investigate the effect of mixing conditions on properties of silica-filled rubber for tire tread compounds.[17–19] However, comparison has not yet been made between conventional silica (CSi) and highly dispersible silica (HDSi), a new generation of silica claimed to be easily dispersible because of its greater branched structure (higher structure) leading to the higher shear force during the mixing process.[20]

It is therefore the intention of this work to compare the effect of silanization temperature on properties of silica-filled solution polymerized styrene butadiene rubber (SSBR) reinforced by CSi and HDSi for passenger car tire tread compounds. Comparison of tire performance between CSi-filled and HDSi-filled tread compounds at various silanization temperatures is also reported.

EXPERIMENTAL

Materials

All mixing ingredients were used as-received. Oil extended SSBR (SOLC6450SL with 54.5 of ML(1 + 4)@100°C, 27.1% of treated distillate aromatic extract (TDAE) content, 34.6% of styrene content and 40.1% of vinyl content) was produced by Kumho Petrochemical, South Korea. HDSi (Zeosil 1165MP with the average primary particle size of 20 nm and BET specific surface area of 153 m^2/g) was manufactured by Rhodia Silica Korea, South Korea. CSi (Tokusil 255), having the average primary particle size of 20 nm and BET specific surface area of 166 m^2/g, was obtained from OSC Siam Silica, Thailand. TESPT (Si-69) was supplied by Innova (Tianjin) Chemical, China. N-(1,3-dimethylbutyl)-N′-phenyl-p-phenylenediamine (6PPD), 2,2,4-trimethyl-1,2-dihydroquinoline (TMQ) and N-tert-butyl-2-benzothiazyl sulfenamide (TBBS) were purchased from Monflex Pte., Singapore. Other chemicals were obtained from suppliers in Thailand. Zinc oxide (ZnO, white seal) was supplied by Thai-Lysaght. Stearic acid was purchased from Kij Paiboon Chemical, Part. Paraffin wax was supplied by Petch Thai Chemical. TDAE oil was obtained from PSP Specialties. Tetrabenzylthiuram disulfide (TBzTD) and sulfur were purchased from Behn Meyer Chemicals (Thailand) and The Siam Chemical Public, respectively.

Preparation and Testing of Rubber Compounds

The formulation employed in this study is given in Table I. Mixing was carried out using a laboratory-sized internal mixer (Brabender Plasticorder 350E, Germany). Fill factor and rotor speed were kept constant at 0.75 and 40 rpm, respectively. Three-step mixing was used in this experiment. In the first step, SSBR was mixed with all ingredients, except for curatives (TBBS, TBzTD and sulfur), at the mixing temperature of 60°C for 10 min to gain satisfactory degree of filler dispersion. The compounds were then sheeted on a two-roll mill (Labtech LRM150, Thailand) and cooled down to the room temperature. In the second step, the so-called silanization step, the compounds were re-mixed at high temperature (the silanization temperature was varied from 120°C to 160°C) for 6 min to promote the silanization reaction between TESPT and silica. Again, the compounds were then sheeted and cooled down to room temperature. In the final step, the compounds were mixed with the curatives at the mixing temperature of 60°C for 3 min. After mixing, the compounds were sheeted and kept overnight at room temperature prior to testing.

Table I. The Compound Formulation (Unit: Parts per Hundred Rubber; phr)

Ingredient	Content (phr)
SSBR	137.5
ZnO	3.0
Stearic acid	2.0
6PPD	1.5
TMQ	1.0
Paraffin wax	2.0
TDAE	10.0
Silica (Zeosil 1165MP or Tokusil 255)	80.0
TESPT (8% w/w of silica)	6.4
TBBS	1.2
TBzTD	0.2
Sulfur	2.2

Measurement of Mooney viscosity (ML(1 + 4)@100°C) was carried out in accordance with ISO 289-1 using a Mooney viscometer (TechPro viscTECH+, USA). Cure characteristics were investigated using a moving die rheometer (MDR, TechPro MD+, USA) at 160°C following ISO 6502. Payne effect was determined by the use of a rubber process analyzer (RPA, Alpha Technologies RPA2000, USA) at frequency of 1.7 Hz and temperature of 100°C. The dynamic strain was varied from 0.56% to 100.02%. The difference between storage moduli at 0.56% and 100.02% (or $\Delta G'$) was used to determine the Payne magnitude of the compounds. Measurement of bound rubber content (BRC) was carried out by extracting the unbound rubber with toluene. Approximately 0.5 g of rubber test piece was extracted by 100 mL of toluene for 168 h at room temperature. After filtering with filter paper, the insoluble part was dried in an oven at 70°C until a constant weight was gained. The BRC was calculated by the following equation:

Table II. Dump Temperature and Temperature Rise of the Compounds

	HDSi		CSi	
Silanization temperature (°C)	Dump temperature (°C)	Temperature rise (°C)	Dump temperature (°C)	Temperature rise (°C)
120	135	15	134	14
130	142	12	142	12
140	147	7	146	6
150	154	4	154	4
160	166	6	165	5

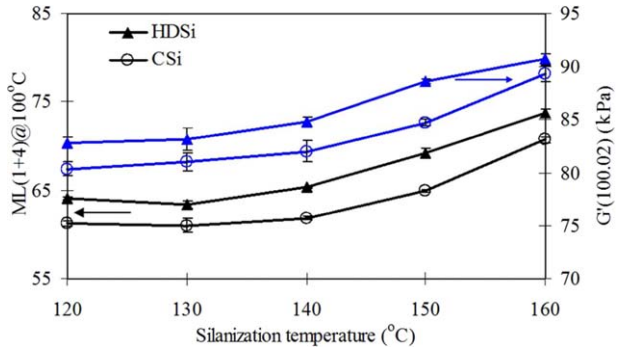

Figure 1. G' at high strain and Mooney viscosity of the compounds. [Color figure can be viewed in the online issue, which is available at wileyonlinelibrary.com.]

$$\text{BRC}\,(\%) = \left[\frac{(W_d - F)}{R}\right] \times 100 \qquad (1)$$

where W_d is the weight of dry gel, F is the weight of filler in the test piece, and R is the weight of rubber in the test piece. It is generally accepted that BRC measured at room temperature is formed by both physical and chemical interactions.[21] As physically bound rubber could be destroyed at high temperature,[22] the amount of chemically bound rubber could therefore be determined by the above procedure, except that, the extraction was carried out at 85°C for 36 h. Determination of molecular weight of the rubber matrix was carried out using gel permeation chromatography technique (GPC, WatersTM 150-CV plus, USA).

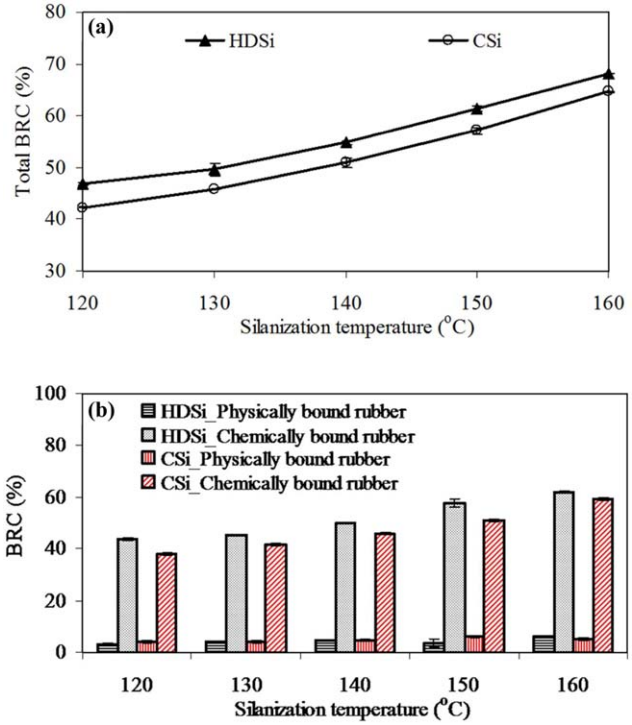

Figure 2. Types of BRC of the compounds prepared with various silanization temperature: (a) total BRC and (b) physically and chemically bound rubber. [Color figure can be viewed in the online issue, which is available at wileyonlinelibrary.com.]

Approximately 5 mg of rubber compound was dissolved in 5 mL of tetrahydrofuran (THF) for 5 days. The solution (100 μL) was filtrated prior to being injected into the GPC instrument. The mobile phase was THF, and the flow rate of 1 mm/min was used.

Testing of Rubber Vulcanizates

Vulcanization was carried out in a hydraulic hot press (Wabash MPI G30-15-0X, USA) at 160°C based on the optimum cure time measured from MDR. Cross-link density was reported in terms of a swelling ratio. Rubber test pieces were immersed in toluene for 5 days. After the immersion, the specimens were blotted off with filter paper prior to the determination of mass change. The swelling ratio was calculated based on the equation as follows:

$$\text{Swelling ratio}\ (\%) = \frac{(W_1 - W_0)}{W_0} \times 100 \qquad (2)$$

where W_0 and W_1 are the weights of the test specimen before and after swelling, respectively.

Determination of hardness was carried out using a Shore A durometer (Wallace H17A, UK) according to ISO 7619 Part 1. Tensile properties were determined using a universal testing machine (Instron 3366 series, USA) following ISO 37 (die type 1). Abrasion resistance test was performed by Akron abrasion tester (Gotech GT-7012-A, Taiwan) according to BS 903: Part A9, Method B. Heat build-up (HBU) was evaluated in terms of temperature rise at specimen base following ISO 4666 by the use of a Goodrich flexometer (BF Goodrich Model II, USA). After the HBU test, dynamic set was also evaluated. The specimens were taken from the test chamber and left at room temperature for 30 min before the measurement of their final height. The dynamic set is calculated using the following equation.

$$\text{Dynamic set}\ (\%) = \frac{(H_0 - H_f)}{H_0} \times 100 \qquad (3)$$

where H_0 and H_f are the original and final heights of the specimen, respectively. Dynamic properties were evaluated in tension mode using a dynamic mechanical thermal analyzer (DMTA: Gabo Qualimeter Eplexor 25N, Germany). For temperature sweep test, the test conditions were as follows: static strain of 1%, dynamic strain of 0.15%, frequency of 10 Hz, and heating rate of 2°C/min. The temperature was scanned from −60°C to

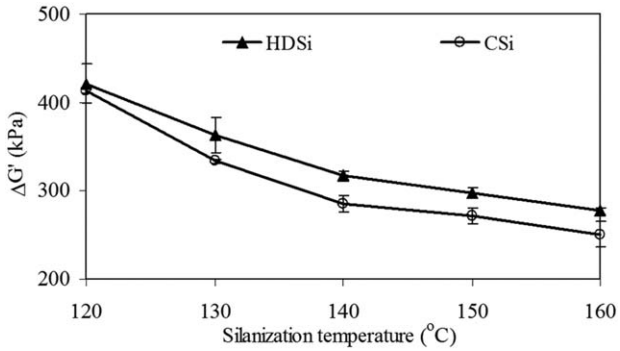

Figure 3. Payne effect of the compounds.

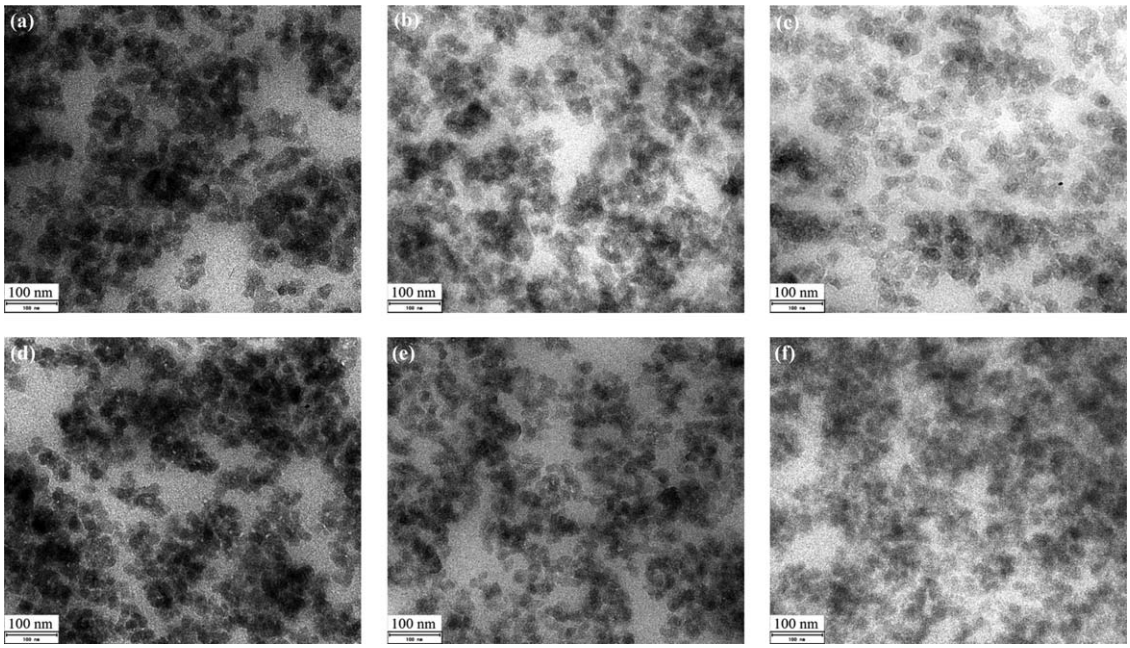

Figure 4. TEM micrographs (x20,000) of the silica-filled vulcanizates at various silanization temperatures: (a) HDSi_120°C, (b) HDSi_140°C, (c) HDSi_160°C, (d) CSi_120°C, (e) CSi_140°C, and (f) CSi_160°C.

80°C. To perform the strain sweep test, the static strain and frequency were set at 12% and 10 Hz, respectively. The dynamic strain was varied from 0.03% to 10% at both 0°C and 60°C. The degree of filler dispersion was examined by transmission electron microscopy (TEM, JEOL JEM-2010, Japan) under an accelerating voltage of 200 kV. TEM images were taken on the ultra-thin sections of the specimens prepared under cryogenic condition at −70°C using an ultra-microtome (Leica EM FCS, Austria).

RESULTS AND DISCUSSION

Mixing Behavior in Silanization Step

Table II represents dump temperature and temperature rise of the compounds recorded during the silanization step. As expected, the dump temperature increases continuously with increasing silanization temperature whereas the temperature rise remarkably decreases with increasing silanization temperature up to 140°C and then tends to level off. Such decrease in temperature rise with increasing silanization temperature is explained as follows; with increasing silanization temperature, bulk viscosity is reduced and, thus the shear heating during the mixing process. However, at high silanization temperatures (≥140°C), the effect of scorching phenomenon, because of the released sulfur from TESPT, on bulk viscosity is more dominant leading to the insignificant changes of viscosity and, thus, temperature rise. Similar observation is also reported in which the scorch could be found in the SSBR/BR blend when mixed with TESPT at high temperature.[17] It is also found that dump temperature and temperature rise are independent of silica type.

Compound and Vulcanizate Properties

Figure 1 discloses storage modulus (G') at high strain of 100% measured by RPA2000 and Mooney viscosity of the compounds. As can be seen, G' at high strain and Mooney viscosity increase slightly with increasing silanization temperature up to 140°C and then dramatically increase thereafter. The possible explanations are given to the enhancement in magnitude of rubber–filler interaction (see Figure 2) and the scorching phenomenon induced by TESPT which is more pronounced at high temperature as previously discussed. The findings imply the decreased mobility of rubber molecules with increasing silanization temperature. Results presented in

Table III. Cure Characteristics of the Compounds

	HDSi		CSi	
Silanization temperature (°C)	t_s1 (min)	t_c90 (min)	t_s1 (min)	t_c90 (min)
120	0.85 ± 0.04	15.45 ± 0.16	0.54 ± 0.04	15.02 ± 0.12
130	0.86 ± 0.02	16.55 ± 0.06	0.82 ± 0.03	16.63 ± 0.45
140	1.11 ± 0.04	17.56 ± 0.05	1.00 ± 0.04	18.26 ± 0.28
150	1.43 ± 0.09	19.40 ± 0.06	1.26 ± 0.05	19.32 ± 0.49
160	2.46 ± 0.01	20.88 ± 0.08	2.03 ± 0.06	21.60 ± 0.59

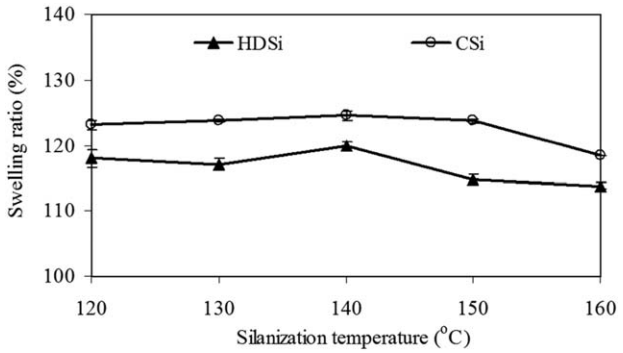

Figure 5. Relationship between swelling ratio of the vulcanizates and silanization temperature.

Figure 1 also reveal that HDSi-filled compounds possess considerably higher G' at high strain and Mooney viscosity than CSi-filled compounds. The greater rubber–filler interaction and the higher structure level of HDSi could be the reasonable explanations for this finding.

The relationship between BRC and silanization temperature is given in Figure 2. With increasing silanization temperature, both total BRC and chemically bound rubber consecutively increase. Moreover, the portion of chemically bound rubber is obviously higher than that of physically bound rubber. The results imply that the increased silanization temperature can improve the rubber–filler interaction via the coupling reaction, resulting in the strong chemical interaction between rubber and silica. At a given silanization temperature, HDSi provides greater total BRC and chemically bound rubber content, compared to CSi, suggesting the stronger rubber–filler interaction.

Figure 3 depicts Payne effect of the compounds as a function of silanization temperature. Generally, the greater the Payne effect magnitude, the larger the amount of filler network. As expected, with increasing silanization temperature, the Payne magnitude tends to decrease revealing a reduction in filler network caused by the silanization reaction between ethoxysilyl groups of TESPT and silanol groups on silica surfaces. Since the Payne magnitude is greater in the system filled with HDSi, it could be said that HDSi gives stronger filler–filler interaction than CSi, possibly because of its higher structure.

Figure 4 represents TEM micrographs (×20,000) of the vulcanizates. As expected, the dispersion of silica is improved with increasing silanization temperature regardless of silica type. The results are in good accordance with the Payne effect results. The decreased hydrophilicity of silica surfaces after silanization reaction and the enhancement in rubber–filler interaction via the coupling reaction are believed to be responsible for such finding. Unexpectedly, at any given silanization temperature, both HDSi and CSi demonstrate comparable degree of dispersion. The relatively long mixing time used in this experiment which might override the silica type effect is proposed to explain such findings.

Cure characteristics of the compounds are exhibited in Table III. It can evidently be seen that both scorch time (t_s1) and optimum cure time (t_c90) tend to increase with increasing silanization temperature, attributed mainly to the reduced concentration of curatives in the rubber matrix caused by the increase in the amount of mobilized rubber because of the improved filler dispersion. Results also reveal that cure characteristics of the compounds are independent of silica type.

The relationship between swelling ratio and silanization temperature is shown in Figure 5. Change of swelling ratio is not noticeable with increasing silanization temperature up to 140°C. However, at higher silanization temperatures, swelling ratio tends to decrease significantly due possibly to the increased rubber–filler interaction. It has been reported that the tightly bound rubber could restrict the rubber molecules from swelling and, thus, could behave as cross-link points in rubber vulcanizates.[23] Again, as HDSi provides considerably higher magnitude of rubber–filler interaction, the HDSi-filled vulcanizates therefore shows lower swelling ratio than the CSi-filled vulcanizates.

Table IV summarizes mechanical properties of the vulcanizates. In spite of the enhanced rubber–filler interaction and cross-link density (particularly at silanization temperature >140°C), the reduction in hardness with increasing silanization temperature is found, possibly because of the dominant effects of the reduced magnitude of filler network and molecular weight of rubber matrix (see Table V), as measured by a GPC technique. The results obtained from GPC exhibit that the molecular weight of rubber in the compounds tends to decrease with increasing silanization temperature, revealing the thermal degradation of rubber at high silanization temperature. Because of the combined consequences of the greater magnitudes of rubber–filler interaction, filler network, and cross-link density, the HDSi-filled vulcanizate shows significantly higher hardness than the CSi-filled vulcanizate.

Table IV. Mechanical Properties of the Vulcanizates

Silanization temperature (°C)	HDSi				CSi			
	Hardness (Shore A)	TS (MPa)	M100 (MPa)	Volume loss (mm^3)	Hardness (Shore A)	TS (MPa)	M100 (MPa)	Volume loss (mm^3)
120	69.3 ± 0.6	19.8 ± 0.2	3.2 ± 0.1	39.2 ± 0.5	67.4 ± 0.7	20.4 ± 1.7	3.0 ± 0.1	30.5 ± 0.8
130	67.1 ± 0.2	20.3 ± 0.7	3.3 ± 0.1	38.4 ± 1.8	66.1 ± 0.4	19.7 ± 1.9	3.0 ± 0.1	29.9 ± 1.0
140	66.1 ± 0.4	20.2 ± 1.0	3.3 ± 0.1	35.5 ± 0.8	64.7 ± 0.6	19.0 ± 1.0	3.1 ± 0.2	28.8 ± 0.7
150	63.9 ± 0.4	19.8 ± 0.6	3.8 ± 0.1	32.2 ± 0.7	63.4 ± 0.2	19.1 ± 0.8	3.1 ± 0.1	25.7 ± 0.5
160	63.0 ± 0.5	19.8 ± 0.7	4.0 ± 0.1	30.5 ± 0.8	61.3 ± 0.3	20.6 ± 1.4	3.8 ± 0.3	25.4 ± 0.8

Table V. Molecular Weight of Rubber Portion in the Compounds

Silanization temperature (°C)	HDSi			CSi		
	M_n (Daltons)	M_w (Daltons)	M_p (Daltons)	M_n (Daltons)	M_w (Daltons)	M_p (Daltons)
120	440,709	713,072	855,512	447,183	708,343	859,915
130	405,666	691,584	846,044	411,515	710,093	870,939
140	347,774	630,732	799,340	356,733	670,704	840,166
150	341,641	616,347	758,408	354,700	640,499	804,040
160	325,272	541,949	667,836	361,976	635,933	756,510

Unexpectedly, tensile strength (TS) does not significantly change with increasing silanization temperature, possibly because of the counter-balance between the reduced molecular weight and the increased filler dispersion and rubber–filler interaction. Results also suggest little effect of silica type on tensile strength.

Unlike hardness, modulus at 100% strain (M100) is found to increase with increasing silanization temperature. This might be attributed to the dominant effects of the enhanced cross-link density and rubber–filler interaction. As expected, the higher modulus is observed in the HDSi-filled systems, because of the greater cross-link density and stronger rubber–filler interaction.

Results presented in Table IV also show that, with increasing silanization temperature, the volume loss is found to decrease meaning the improved abrasion resistance. The enhancements of rubber–filler interaction and degree of filler dispersion could be used to explain the results. Unexpectedly, the greater abrasion resistance is observed in the CSi-filled vulcanizates.

The effect of silanization temperature on HBU and dynamic set is displayed in Table VI. Because of the reduced magnitude of filler network and the increased rubber–filler interaction and cross-link density, HBU and dynamic set decrease slightly with increasing silanization temperature. Results also suggest that the silica type does not significantly influence HBU and dynamic set of the vulcanizates.

Figure 6 illustrates effect of silanization temperature on loss factor (tan δ). Glass transition temperature (T_g), tan δ_{max} and tan δ area extracted from Figure 6 are summarized in Table VII. The T_g of the vulcanizates tends to increase with increasing silanization temperature. This is understandable because, with increasing silanization temperature, the magnitude of rubber–filler interaction is enhanced, leading to the increased restriction of the molecular motion. It is also found that the values of tan δ_{max} and tan δ area increase consecutively with increasing silanization temperature indicating the greater amount of rubber chains participating in the glass transition which results from the improved filler dispersion. It has been reported that the tan δ value of filled polymer can be calculated using the following equation[24,25]:

$$\tan \delta_f = \frac{\tan \delta_u}{(1+B\varphi)} \quad (4)$$

where tan δ_f and tan δ_u are the tan δ_{max} values of filled and unfilled polymer, respectively, B is the phenomenological

Table VI. Heat Build-Up (HBU) and Dynamic Set of the Vulcanizates

Silanization temperature (°C)	HDSi		CSi	
	Heat build-up (°C)	Dynamic set (%)	Heat build-up (°C)	Dynamic set (%)
120	13.5 ± 0.5	4.64 ± 0.34	13.0 ± 0.0	4.39 ± 0.50
130	13.0 ± 0.0	4.50 ± 0.14	13.0 ± 0.0	4.44 ± 0.12
140	13.0 ± 0.0	4.30 ± 0.09	13.0 ± 0.0	4.18 ± 0.37
150	13.0 ± 0.0	4.37 ± 0.18	12.5 ± 0.7	4.00 ± 0.11
160	12.5 ± 0.7	3.76 ± 0.06	12.0 ± 0.0	3.68 ± 0.12

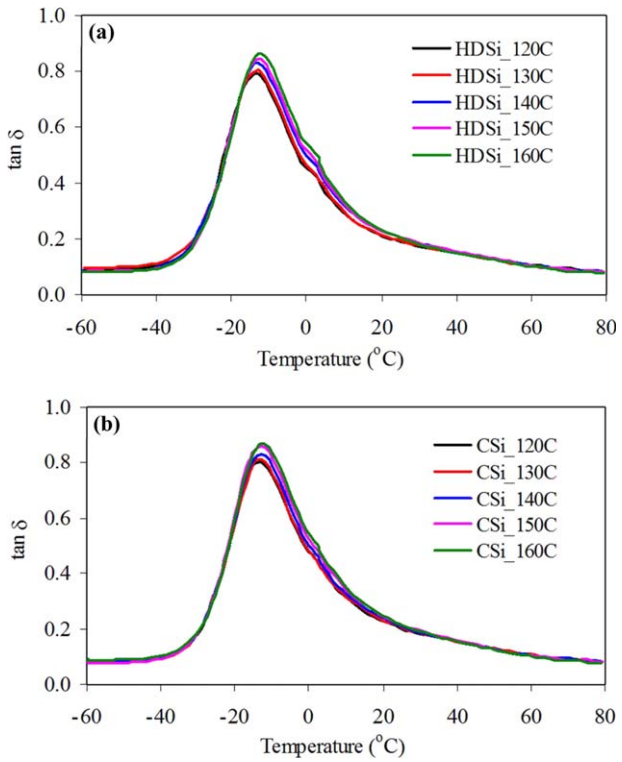

Figure 6. Loss factor (tan δ) as a function of test temperature of the vulcanizates at various silanization temperatures: (a) HDSi and (b) CSi. [Color figure can be viewed in the online issue, which is available at wileyonlinelibrary.com.]

Table VII. Glass Transition Temperature (T_g), Tan δ_{max} and Tan δ Area of the Vulcanizates

	HDSi			CSi		
Silanization temperature (°C)	T_g (°C)	tanδ_{max}	tanδ area (°C)	T_g (°C)	tanδ_{max}	tanδ area (°C)
120	−14.0	0.787	15.36	−13.7	0.787	15.95
130	−13.5	0.803	15.71	−13.3	0.802	16.06
140	−12.9	0.828	16.35	−12.8	0.828	16.55
150	−12.8	0.842	16.77	−12.6	0.840	17.42
160	−12.2	0.862	17.35	−12.1	0.864	17.38

interaction parameter which is directly related to the polymer–filler interaction, and φ is the effective volume fraction of filler. As tan δ_{max} increases continuously with increasing silanization temperature, the results indicate that the multiple of $B\varphi$ must be decreased. However, since B is increased with increasing silanization temperature as evidenced from the BRC results, φ must be greatly decreased. The reduction of φ with increasing silanization temperature arises from the improved filler dispersion. Results also demonstrate that silica type provides little effect on T_g and tan δ_{max} values. However, it is observed that CSi gives slightly higher tan δ area than HDSi, possibly attributed to its lower structure and, thus, trapped rubber.

In tire application, tan δ values at 0°C and 60°C are usually used to predict WG and RR, respectively.[2,7,8] The higher the tan δ at 0°C, the better the WG of vulcanizates. The lower the tan δ at 60°C, the lower the RR of vulcanizates. The tan δ values of the vulcanizates as a function of dynamic strain from 0.03% to 10% at 0°C are represented in Figure 7. It is found that, at a given strain, WG of the vulcanizates as indicated from the tan δ at 0°C increases continuously with increasing silanization temperature. Unexpectedly, both HDSi and CSi demonstrate comparable WG. Results in Figure 7 also show that the tan δ value increases with increasing dynamic strain up to 3% strain and, then decreases afterwards. The initial increase of tan δ is caused mainly by the increased destruction of filler network whereas the reduced tanδ at high strain results from the disappearance of filler network.

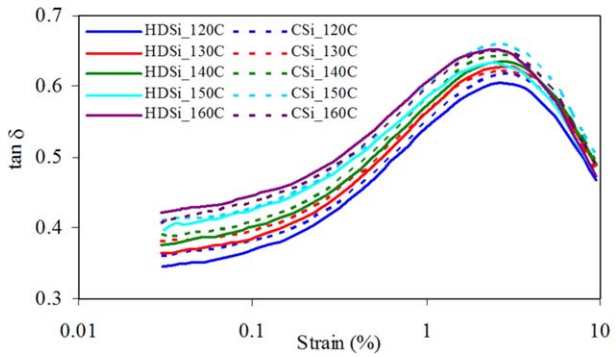

Figure 7. Loss factor (tan δ) as a function of dynamic strain at 0°C of the vulcanizates. [Color figure can be viewed in the online issue, which is available at wileyonlinelibrary.com.]

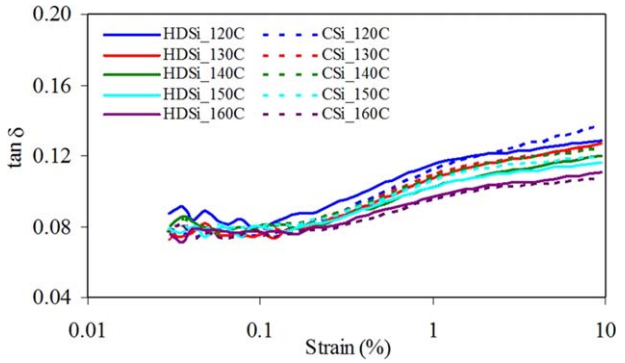

Figure 8. Loss factor (tan δ) as a function of dynamic strain at 60°C of the vulcanizates. [Color figure can be viewed in the online issue, which is available at wileyonlinelibrary.com.]

Figure 8 discloses the tan δ at 60°C of the vulcanizates as a function of dynamic strain. As expected, RR tends to decrease with increasing silanization temperature. Explanation is given by the improved rubber–filler interaction, leading to the lower magnitude of molecular slippage on the filler surfaces during the deformation and, hence, the lower energy dissipation. Similar to WG, RR of the vulcanizates is independent of the silica type. Although HDSi gives greater rubber–filler interaction and cross-link density than CSi, in the meantime, it provides higher

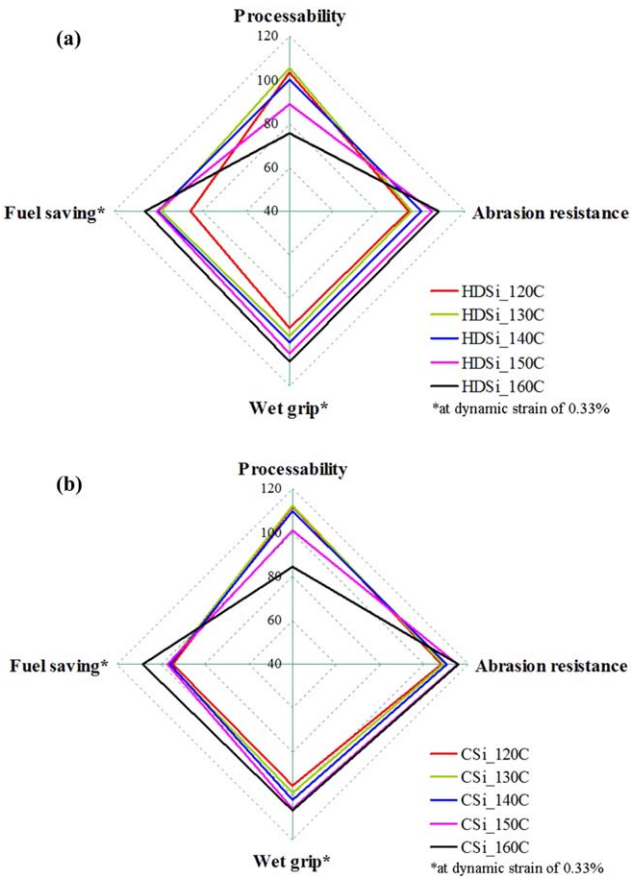

Figure 9. Normalized graph of processability and tire performance at various silanization temperatures (a) HDSi and (b) CSi. [Color figure can be viewed in the online issue, which is available at wileyonlinelibrary.com.]

magnitude of filler network available for energy dissipation. HDSi and CSi therefore give comparable RR.

Figure 9 represents the effect of silanization temperature on processability (evaluated from Mooney viscosity) and tire performance in terms of the normalized graph. Clearly, the balanced properties are found at the silanization temperature of 140°C.

CONCLUSIONS

With increasing silanization temperature, the tire performance, e.g., WG, RR, and abrasion resistance are significantly improved with the sacrifice of processability. Such improvements arise from the enhanced rubber–filler interaction, improved filler dispersion and increased cross-link density. Overall, the silanization temperature of 140°C provides a good balance between tire performance and processability. Surprisingly, HDSi and CSi demonstrate comparable degree of filler dispersion, scorch time (t_s1), optimum cure time (t_c90), tensile strength, HBU, dynamic set, including WG and RR. The results reveal that silica type has little effect on tire performance, as long as the sufficiently long mixing time is employed.

ACKNOWLEDGMENTS

The authors thank the Thailand Research Fund (TRF) through the Research and Researchers for Industries (RRi) and Siam Rubber Ltd., Part (Grant PHD56I0074) for financial support throughout this study.

REFERENCES

1. Hirata, Y.; Kondo, H.; Ozawa, Y. In Chemistry, Manufacture and Applications of Natural Rubber; Kohjiya, S.; Ikeda, Y., Eds.; Woodhead Publishing: UK, **2014**; Chapter 12, p 325.
2. Muraki, T.; Ishikawa, Y. U.S. Patent 5,500,482 (**1996**).
3. Rao, G. V.; Mouli, S. C.; Boddeti, N. K. *Int. J. Eng. Technol.* **2010**, *2*, 87.
4. Wang, Y. X.; Wu, Y. P.; Li, W. J.; Zhang, L. Q. *Appl. Surf. Sci.* **2011**, *257*, 2058.
5. Karak, N.; Gupta, B. R. K. *Kautsch. Gummi Kunstst.* **2000**, *53*, 30.
6. Saeed, F.; Ansarifar, A.; Ellis, R. J.; Haile-Meskel, Y.; Irfan, M. S. *J. Appl. Polym. Sci.* **2012**, *123*, 1518.
7. Liu, X.; Zhao, S.; Zhang, X.; Li, X.; Bai, Y. *Polymer* **2014**, *55*, 1964.
8. Ko, J. Y.; Prakashan, K.; Kim, J. K. *J. Elastom. Plast.* **2012**, *44*, 549.
9. Lee, H. G.; Kim, H. S.; Cho, S. T.; Jung, I. T.; Cho, C. T. *Asian J. Chem.* **2013**, *25*, 5251.
10. Zafarmehrabian, R.; Gangali, S. T.; Ghoreishy, M. H. R.; Davallu, M. E. *J. Chem.* **2012**, *9*,
11. Rattanasom, N.; Saowapark, T.; Deeprasertkul, C. *Polym. Test.* **2007**, *26*, 369.
12. Liu, Y.; Li, L.; Wang, Q. *J. Appl. Polym. Sci.* **2010**, *118*, 1111.
13. Ayippadath Gopi, J.; Patel, S.; Chandra, A.; Tripathy, D. *J. Polym. Res.* **2011**, *18*, 1625.
14. Rauline, R. Patent EP 0 501227 A1 (**1992**).
15. Waddell, W. H.; Evans, L. R. In Rubber Technology: Compounding and Testing for Performance; Dick, J. S., Ed.; Hanser Publishers: Munich, **2001**; Chapter 13, p 325.
16. Goerl, U.; Hunsche, A.; Mueller, A.; Koban, H. G. *Rubber Chem. Technol.* **1997**, *70*, 608.
17. Reuvekamp, L. A. E. M.; Brinke, J. W.; Swaaij, P. J.; Noordermeer, J. W. M. *Kautsch. Gummi Kunstst.* **2002**, *55*, 41.
18. Kaewsakul, W.; Sahakaro, K.; Dierkes, W. K.; Noordermeer, J. W. M. *Rubber Chem. Technol.* **2012**, *85*, 277.
19. Wolff, S. *Rubber Chem. Technol.* **1982**, *55*, 967.
20. Chakraborty, S.; Shah, D.; Silica, M. *Rubber World* **2013**, 37. pp
21. Wolff, S.; Wang, M. J.; Tan, E. H. *Chem. Technol.* **1993**, *66*, 163.
22. Wolff, S. *Rubber Chem. Technol.* **1996**, *69*, 325.
23. Valentín, J. L.; Mora-Barrantes, I.; Carretero-González, J.; López-Manchado, M. A.; Sotta, P.; Long, D. R.; Saalwächter, K. *Macromolecules* **2010**, *43*, 334.
24. Ziegel, K. D.; Romanov, A. *J. Appl. Polym. Sci.* **1973**, *17*, 1119.
25. Qu, L.; Yu, G.; Xie, X.; Wang, L.; Li, J.; Zhao, Q. *Polym. Compos.* **2013**, *34*, 1575.